JOURNAL OF APPLIED ELECTROCHEMISTRY **28** (1998) 381–385

Electrochemical investigations of bare and Pd-coated $LaNi_{4.25}Al_{0.75}$ electrodes in alkaline solution

G. ZHENG, B. N. POPOV, R. E. WHITE

Center for Electrochemical Engineering, Department of Chemical Engineering, University of South Carolina, Columbia, SC 29208, USA

Received 16 September 1996; revised 10 May 1997

Electrochemical investigations were carried out on electrodes made from both bare and Pd-coated $LaNi_{4.25}Al_{0.75}$ particles. Experimental results showed that the Pd-coating significantly decreases the electrode resistance and increases the electrode discharge capacity. The electrochemical impedance spectroscopy technique was used to determine various resistive components in the electrodes and electrolyte by fitting an equivalent circuit to the experimental data. The results indicated that an electrode made from the Pd-coated alloy has much less ohmic resistance (particle-to-particle contact resistance and current collector to electrode pellet contact resistance) compared to the electrodes made from bare alloy.

Keywords: *Pd-coated electrodes*, *metal–hydride batteries*, *microencapsulation*

List of symbols

C	capacitance (F)
d_{Pd}	thickness of palladium layer (cm)
F	Faraday's constant ($96\,487\ C\ mol^{-1}$)
i	current density per unit of mass ($A\ g^{-1}$)
i_o	exchange current density per unit of mass ($A\ g^{-1}$)
R	gas constant ($8.3144\ J\ mol^{-1}\ K^{-1}$)
R_{el}	electrolyte resistance (Ω)
R_{cp}	current collector to pellet contact resistance (Ωg)
R_p	polarization resistance (Ωg)
R_{pp}	particle to particle contact resistance (Ωg)
$R_{t(ac)}$	total resistance determined from a.c. impedance method (Ωg)
$R_{t(p)}$	total resistance determined from linear polarization curves (Ωg)
R_T	resistance (Ωg)
R_w	Warburg impedance (Ωg)
T	temperature (K)

Greek characters

η	overpotential (V)
γ_{Pd}	density of palladium ($12.02\ g\ cm^{-3}$)
γ_{alloy}	density of the alloy ($7.04\ g\ cm^{-3}$)

1. Introduction

Pd and its alloys are resistant to corrosion in alkaline electrolytes and have a high degradation resistance for the charge–discharge process. Consequently they should have a high degree of utilization as the negative electrodes for metal–hydride batteries [1, 2]. However, in commercially produced battery systems, Pd and Pd alloy hydride electrodes are unlikely to be used because of their high cost relative to AB_5 type mischemetal based compounds [3]. Recently, microencapsulation of alloy particles used to prepare electrodes has been carried out to prevent oxidation and disintegration of the alloy, which leads to better performance of the electrode [4]. An attempt was made in this study to optimize the performance of the alloy by microencapsulating $LaNi_{4.25}Al_{0.75}$ alloy with palladium. The performance of the Pd-coated $LaNi_{4.25}Al_{0.75}$ alloy electrode was investigated by electrochemical techniques, and the results were compared with those obtained for the bare alloy electrode.

2. Experimental details

The following procedure was used to prepare a $LaNi_{4.25}Al_{0.75}$ pellet electrode. $LaNi_{4.25}Al_{0.75}$ powder was passed through a 230 mesh sieve, which gave a particle size of less than 60 μm. These $LaNi_{4.25}Al_{0.75}$ alloy particles were microencapsulated with a thin film of palladium by electroless deposition using hypophosphite as a reducing agent. The alloy powder was immersed in an electroless plating solution containing $1.7\ g\ dm^{-3}$ $PdCl_2$, $160\ ml\ dm^{-3}$ NH_4OH (with 28–30% NH_3 content), $26\ g\ dm^{-3}$ NH_4Cl and $10\ g\ dm^{-3}$ $NaH_2PO_2H_2.H_2O$. The electroless palladium plating was carried out by using palladium to alloy ratio by weight of 1 : 5. The plating process was continued until the brownish colour of $PdCl_2$ vanished in the solution. The concentration of Pd before ($1.7\ g\ dm^{-3}$) and after the plating ($0\ g\ dm^{-3}$) was determined by titration [5]. A detailed electroless palladium coating procedure was described previously [6].

0021-891X

The thickness of the palladium layer was estimated from the weight of palladium plated, the density of Pd and the alloy total surface area, (TSA) using Eq. 1:

$$d_{Pd} = \frac{\text{weight of Pd (g)}}{\gamma_{Pd}\,(\text{g cm}^{-3}) \times \text{TSA}\,(\text{cm}^2)} \qquad (1)$$

The density of palladium is 12.02 g cm^{-3}. The TSA of the alloy particles was estimated from the single particle surface area, πD^2, the single volume of the particle, $\pi D^3/6$, and the alloy density to be 284 cm^2 g^{-1}. Both, the particle surface area and the volume of the particle were estimated by assuming an average spherical particle size of 30 μm. The alloy density was estimated to be 7.04 g cm^{-3} from the stoichiometry formula of the alloy. Using Equation 1, and assuming that the palladium coating was uniformly plated, the thickness of the palladium layer was estimated to be 0.5 μm. However, the TSA determined by BET was approximately 800 cm^2 g^{-1} which gives a thickness of 0.21 μm for the palladium layer. Thus, we approximated that the thickness of the deposited palladium layer is in the range from 0.2 to 0.6 μm.

The pellet electrodes were prepared by mixing the $LaNi_{4.25}Al_{0.75}$ alloy powder with 2.5% of PTFE powder followed by hot-pressing the material between two nickel meshes in a cylindrical press. A pellet with a diameter of 0.8 cm was formed at approximately 300 °C using a pressure of 5 t cm^{-2}. The thickness of the pellet was 0.9 mm. The pellet was then inserted between two pieces of Plexiglass holders with small holes on each side. The electrode was immersed in the test cell which was filled with a 6 M KOH electrolyte solution. Pieces of Pt gauze were placed on both sides of the electrode and served as counter electrodes. A sketch of the cell is presented in Fig. 1.

The experiments were carried out using a Hg/HgO reference electrode and using the model 342C Soft-Corr System with the EG&G PAR potentiostat/galvanostat model 273 at 25 °C.

3. Results and discussion

Linear polarization curves for the bare alloy electrode at different states of charge are given in Fig. 2. The

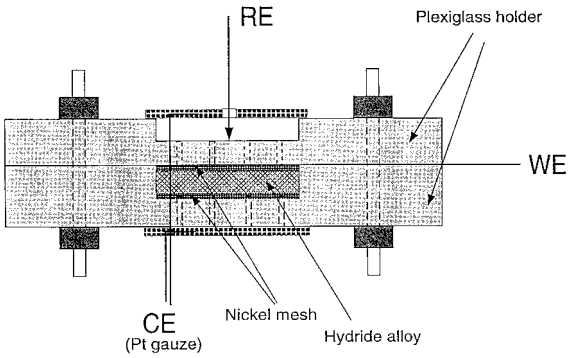

Fig. 1. Sketch of the M–H cell.

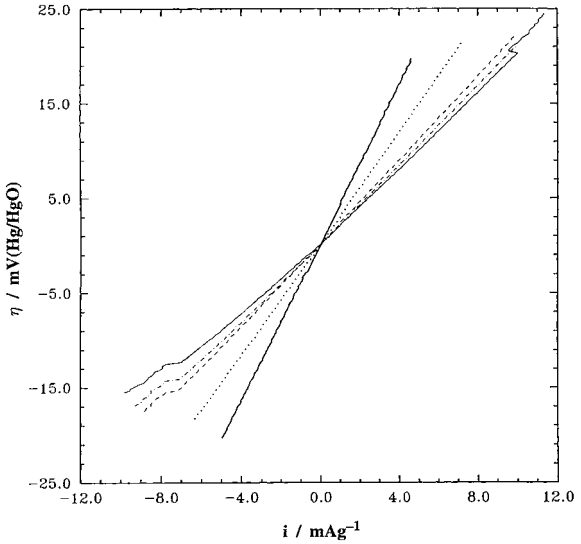

Fig. 2. Linear polarization curves at different state-of-charge for the bare alloy. SOC: (——) 100%, (· · · ·) 75%, (- - -) 50%, (— · —·) 38% and (——) 25%.

curves in Fig. 2 show that the slope of the linear polarization curves decrease with a decrease of the state of charge (hydrogen content in the alloy). The total resistance of the electrode may be determined from the slopes of the curves by using $R_{t(p)} = \eta/i$, where $R_{t(p)}$ is the total resistance from linear polarization curve, η is the overpotential (mV) and i the current density (mA g^{-1}). The corresponding linear polarization curves for the Pd-coated $LaNi_{4.25}Al_{0.75}$ alloy electrode are plotted in Fig. 3. The curves in Fig. 3 show similar behaviour as a function of state of charge to those in Fig. 2. The resistances determined from the slopes of the curves in Figs 2 and 3 are plotted as a function of state of charge in Fig. 4. From Fig. 4 it can be seen that the electrode made from Pd-coated alloy particles has much less resis-

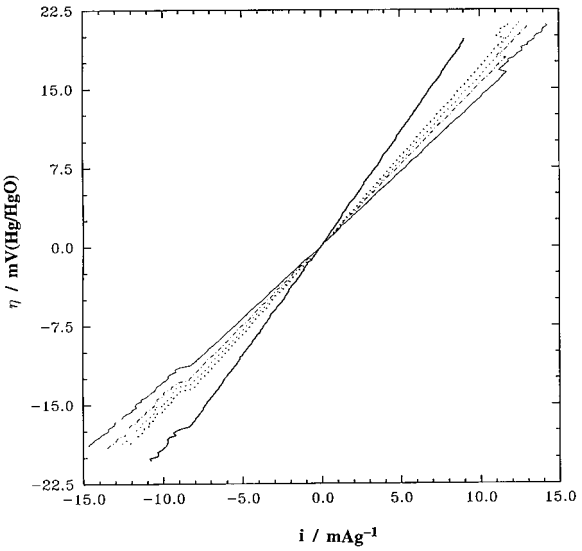

Fig. 3. Linear polarization curves at different state-of-charge for the Pd-coated alloy. SOC: (——) 100%, (· · · ·) 88%, (- - -) 76%, (— · —·) 52% and (——) 29%.

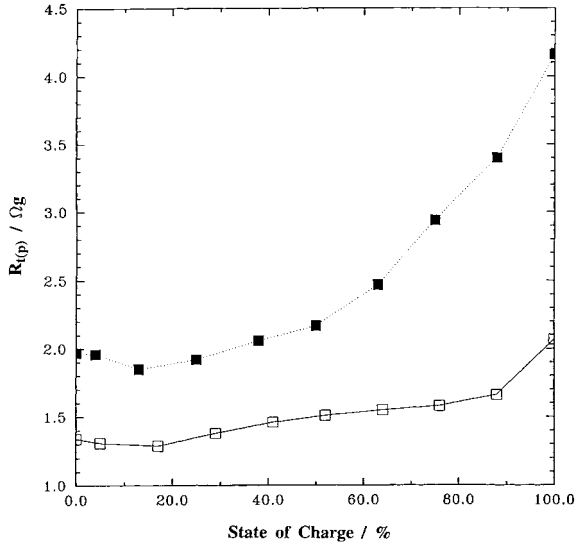

Fig. 4. Total resistances determined from linear polarization curves as a function of the state-of-charge for bare (■) and Pd-coated (□) alloy.

tance than the one made from the bare alloy at the same state of charge.

It was shown previously [6–8] that the total resistance determined from the linear polarization curve ($R_{t(p)}$) is equal to the polarization resistance (R_p) if the ohmic resistance in the electrode is negligible. Thus, the exchange current density of the electrode may be determined by

$$R_p = \frac{RT}{Fi_o} = \frac{\eta}{i} \tag{2}$$

However, when the ohmic resistance is not negligible, R_p in Equation 2 will consist of a sum of the polarization resistance and ohmic resistance. Consequently, the exchange current density will be underestimated. In the present case, the total resistance determined from the linear polarization curve was not equal to the polarization resistance.

Electrochemical impedance spectroscopy (EIS) enables the determination of the polarization resistance and the evaluation of the exchange current density without the interference of any of the ohmic resistance related to alloy particle to particle contact resistance and current collector to pellet contact resistance. EIS experiments were carried out at different states of charge. The impedance data generally covered the frequency range from 0.002 Hz to 100 kHz with an a.c. voltage signal varying by ±5 mV, which ensured the electrode system to be under minimum perturbation. According to Kuriyama *et al.* [9–11] the total resistance is the sum of the following resistances: (i) the electrolyte resistance (R_{el}), (ii) the resistance between the current collector and the electrode pellet (R_{cp}), (iii) the alloy particle to particle contact resistance (R_{pp}) and (iv) the polarization resistance (R_p) which is related to the electrode reaction on the alloy surface and is inversely proportional to the active surface area. The corresponding equivalent circuit is given in Fig. 5, where R_w is the Warburg resistance,

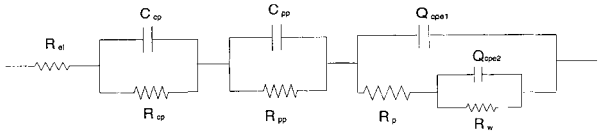

Fig. 5. An equivalent circuit for the metal–hydride electrode.

the *C*s are the capacitances and Q_{cpe1} and Q_{cpe2} are the constant phase elements (CPE) [12].

The Nyquist plots of both bare and Pd-coated electrodes at different states of charge are given in Figs 6 and 7. As shown in these Figures, the total impedance decreases with the decrease of the state of charge, which is consistent with linear polarization results. Further, two semicircles are observed in some of the curves presented in Figs 6 and 7. The semicircle at the low frequency region represents the polarization resistance, while the semicircle at the high frequency region represents the contact resistance between the current collector and the electrode pellet. A third circle exists between these two semicircles and it represents the alloy particle to particle contact resistance. However, at low states of charge (<20%), the two semicircles are not distinguishable due to the overlap of the semicircles. The resistive components may be determined from the EIS data by applying the equivalent circuit shown in Fig. 5. The experimental results shown in Figs 6 and 7 were fitted by using ZView® (a trademark of Scribner and Associates, Inc.). For comparison with the experimental results, the fitted curves were plotted as solid curves.

The various resistive components (polarization resistance, particle to particle contact resistance and current collector to pellet contact resistance) were estimated by fitting the experimental data and are plotted in Figs 8 and 9 as a function of state of charge. Note that the total resistance from a.c. impedance ($R_{t(ac)}$) is the sum of R_p, R_{pp} and R_{cp}. As shown in Figs 8 and 9, the total resistances

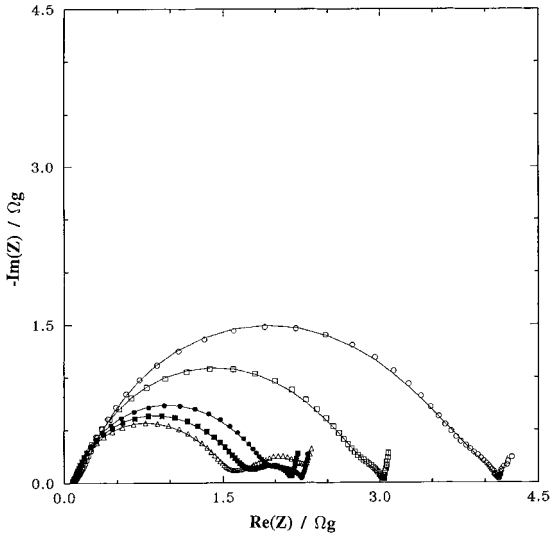

Fig. 6. Nyquist plots at different states-of-charge of bare alloy. SOC: (○) 100%, (□) 75%, (●) 50%, (■) 38% and (△) 25%. Solid lines represent the fitted results.

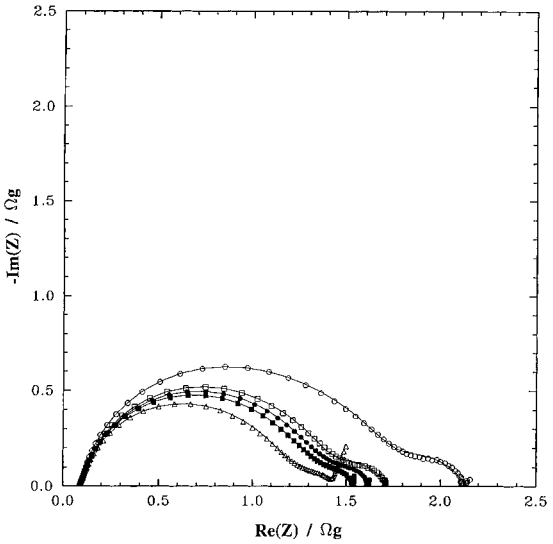

Fig. 7. Nyquist plots at different states-of-charge of Pd-coated alloy. SOC: (○) 100%, (□) 88%, (●) 76%, (■) 52% and (△) 29%. The solid lines are the fitting results.

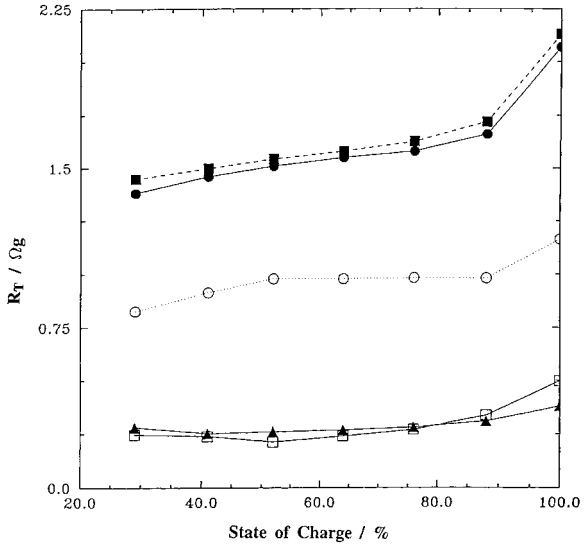

Fig. 9. Resistive components as a function of state-of-charge for Pd-coated alloy. Key: as for Fig. 8.

determined from linear polarization curves ($R_{t(p)}$) at a high state of charge agree with the total resistances obtained from a.c. impedance ($R_{t(ac)}$) measurements. However, with a decrease of the state of charge, the influence of the significant overlaps of the semicircles and the interference of Warburg impedance contribute to the uncertainty of the fitting calculations. Thus, the fittings were not carried out at a state of charge less than 20%.

Figure 8 shows that for the bare alloy current collector to pellet contact resistance R_{cp} has the same magnitude with particle to particle contact resistance R_{pp}. As shown in Fig. 9, for the palladium-coated alloy, the particle to particle contact resistance is much smaller than current collector to pellet resistance. The total ohmic resistance (the sum of R_{cp} and R_{pp}) for the Pd-coated alloy is smaller than that of bare alloy indicating that Pd-coating decreases the contact resistances between the particles.

The polarization resistance estimated for the bare alloy shows a significant increase with a decrease of the state of charge. As shown in Fig. 8, the polarization resistance increases more than 20 times when the SOC decreases from 100% to 25% , indicating that the hydrogen reaction occurs much more easily on $LaNi_{4.25}Al_{0.75}$ hydride surface than on bare $LaNi_{4.25}Al_{0.75}$ alloy surface. As shown in Fig. 9 for Pd-coated alloy, the polarization resistance does not show a strong dependence on the state of charge, indicating that the hydrogen reaction reactivity on both Pd hydride and Pd is the same. The exchange current densities (i_o) for both bare alloy and Pd-coated alloy were calculated from polarization resistance data using Equation 2 and are plotted in Fig. 10 as a function of state of charge. The polarization resistances used to calculate the exchange current densities in Fig. 10 were estimated by fitting the a.c.-impedance results presented in Figs 6 and 7. The

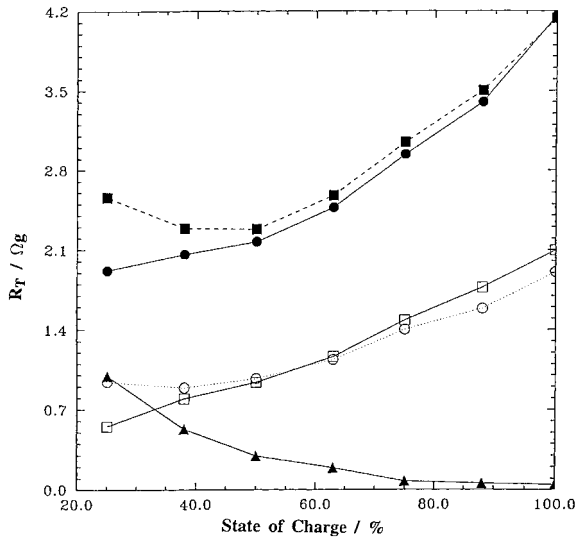

Fig. 8. Resistive components as a function of the state-of-charge for bare alloy. Key: (●) $R_{t(p)}$, (■) $R_{t(ac)}$, (○) R_{cp}, (□) R_{pp} and (▲) R_p.

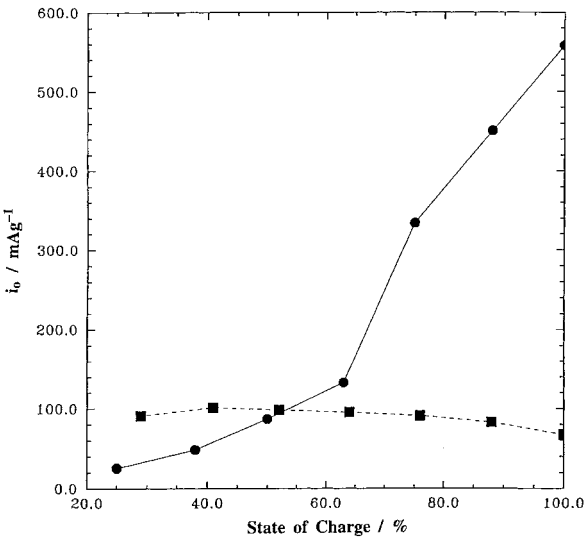

Fig. 10. Exchange current density as a function of state-of-charge for bare (●) and Pd-coated (■) alloy.

exchange current densities on Pd-coated alloy are in the range of 70 to 100 mA g^{-1}. The surface area of the alloy particle determined by BET was approximately 800 $cm^2\ g^{-1}$, which converts the exchange current density into 0.875×10^{-4} to 1.25×10^{-4} A cm^{-2}. This value agrees with the exchange current density value reported in the literature of 10^{-4} A cm^{-2} on Pd surface in 1 M KOH solution [13].

The average experimental discharge capacities (obtained from three different electrodes) of the bare and Pd-coated alloys were estimated to be 125 mA h g^{-1} and 290 mA h g^{-1}, respectively. The theoretical capacity of the alloy was calculated based on the formula of $LaNi_{4.25}Al_{0.75}H_6$ and is 391.8 mA h g^{-1}. Thus, the bare and Pd coated alloy capacities correspond to about 32% and 74% of the theoretical capacity, respectively. Iwakura *et al.* [14] carrying out experiments under hydrogen pressure of 1 atm at 25 °C found that the experimental capacity of bare $LaNi_{4.25}Al_{0.75}$ is 175 mA h g^{-1} at 20 °C. The fact that our experiments were performed under open cell conditions, may explain why the experimental capacity of $LaNi_{4.25}Al_{0.75}$ determined in this study was lower when compared with the value of Iwakura *et al.* [14]. The observed increase of the capacity for Pd-coated alloy may be partly due to the formation of Pd-hydride. Assuming one Pd atom absorbs one hydrogen atom, then Pd will contribute about 50 mA h g^{-1} alloy (Pd to alloy ratio is 1 : 5). The observed increase of the capacity of palladium coated alloy may result from the fact that Pd-coating serves as a barrier which protects the alloy surface from oxidation [14, 15] and active dissolution of aluminium [16]. However, this explanation may justify the observed difference in capacity only if the oxidation of the alloy and the aluminium dissolution reaction occurred during the first charging process. The increase of the capacity of palladium plated alloy may also result from the fact that the hydrogen entry efficiency in the bare alloy (defined as the ratio of the amount of hydrogen entering in bulk of the alloy to form hydride against the amount of hydrogen produced) is much smaller compared with the hydrogen entry efficiency of palladium coated alloy. In other words, the hydrogen atoms on the bare surface tend to recombine and to form hydrogen molecules rather than to diffuse into the alloy and form hydrides.

4. Conclusion

Linear polarization and electrochemical impedance spectroscopy techniques were used to investigate the bare and Pd-coated $LaNi_{4.25}Al_{0.75}$ alloy. The discharge experiments indicated that Pd coating increases the discharge capacity of the bare alloy from 125 to 290 mA h g^{-1}. The results also indicated that Pd-coated alloy decreases the particle to particle contact resistance as well as current collector to pellet contact resistance. The polarization resistance estimated for the bare alloy shows a significant increase with a decrease of the state of charge, indicating that the hydrogen reaction occurs much more easily on a $LaNi_{4.25}Al_{0.75}$ hydride surface than on a pure $LaNi_{4.25}Al_{0.75}$ alloy surface. The exchange current densities (i_o) were calculated from polarization resistance for both the bare alloy and the Pd-coated alloy. The exchange current densities estimated for the Pd-coated alloy were estimated to be 1.25×10^{-4} A cm^{-2} which is in agreement with the exchange current density value reported in the literature of 10^{-4} A cm^{-2} on Pd surface in 1 M KOH solution [13].

Acknowledgement

Financial support by the Exploratory Technology Research (ETR) program, which is supported by the Office of Transportation Technologies (OTT) of the U.S. Department of Energy (DOE), Subcontract 4614610 is acknowledged gratefully.

References

[1] Y. Sakamoto, K. Kuruma and Y. Naritomi, *J. Appl. Electrochemistry* **24** (1994) 38.
[2] Z. Gavra, J. R. Johnson and J. J. Reilly, *J. Less-Common Metals* **172–174** (1991) 107.
[3] T. H. Fuller and J. Newman, *in* 'Modern Aspects of Electrochemistry' Vol. 27 (edited by R. E. White, J. O'M. Bockris and B. E. Conway), Plenum Press, New York (1995), p. 359.
[4] G. Zheng, B. N. Popov and R. E. White, *J. Electrochem. Soc.* **143** (1996) 834.
[5] P. W. Wild, Modern Analysis for Electroplating', Finishing Publications Ltd, Happton Hill, Middlesex, England (1974).
[6] G. Zheng, B. N. Popov and R. E. White, *J. Electrochem. Soc.* **142** (1995) 2695.
[7] *Idem*, *ibid.* **143** (1996) 435.
[8] B. N. Popov, G. Zheng and R. E. White, *J. Appl. Electrochemistry* **26** (1996) 603.
[9] N. Kuriyama, T. Sakai, H. Miyamura, I. Uehara and H. Ishikawa, *J. Alloys and Compounds*, **202** (1993) 183.
[10] N. Kuriyama, T. Sakai, H. Miyamura, I. Uehara and H. Ishikawa, *J. Alloys Compd* **192** (1993) 161.
[11] N. Kuriyama, T. Sakai, H. Miyamura, I. Uehara and H. Ishikawa, *J. Electrochem. Soc.* **139** (1992) L72.
[12] J. R. Macdonald (Ed.), 'Impedance Spectroscopy, Emphasizing Solid Materials and Systems', J. Wiley & Sons, New York (1987).
[13] A. N. Frumkin and N. Aladjalowa, *Acta Physocochim. URRS* **19** (1944) 1.
[14] C. Iwakura, Y. Kajiya and H. Yoneyama, *J. Electrochem. Soc.* **136** (1989) 1351.
[15] T. Sakai, H. Ishikawa, K. Oguro, C. Iwakura and H. Yoneyama, *J. Electrochem. Soc.* **134** (1987) 558.
[16] W. Peng, L. Redey, D. R. Vissers, K. M. Myles, J. Carpanter, J. Richardson and G. Burr, Abstract 64, 189th Electrochemical Society Meeting, The Electrochemical Society, Pennington, NJ, **96–1** (1996) 82.